

Structure of the essential *Haemophilus influenzae* UDP-diacylglucosamine pyrophosphohydrolase LpxH in lipid A biosynthesis

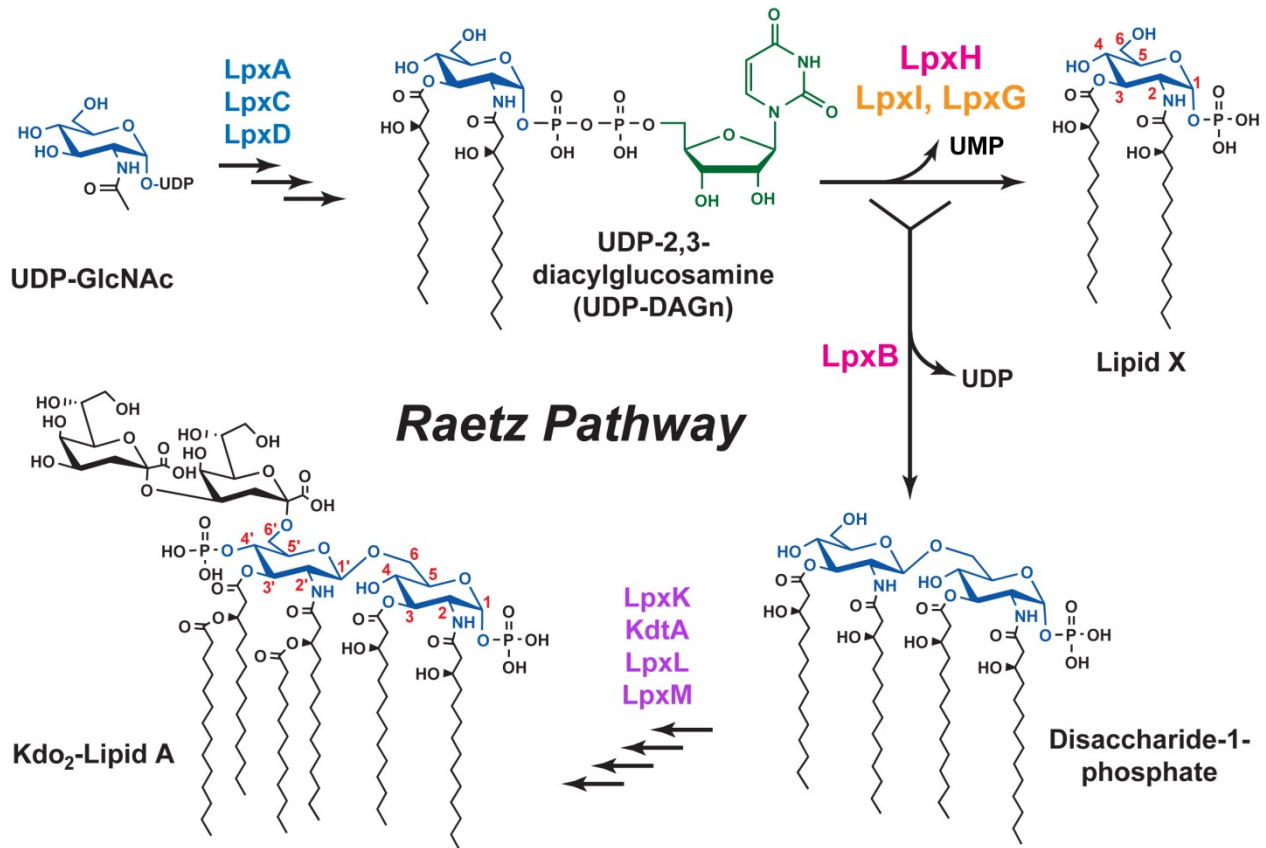
Jae Cho, Chul-Jin Lee, Jinshi Zhao, Hayley E. Young and Pei Zhou

Supplementary Table 1: Data collection and statistics of the LpxH-lipid X complex

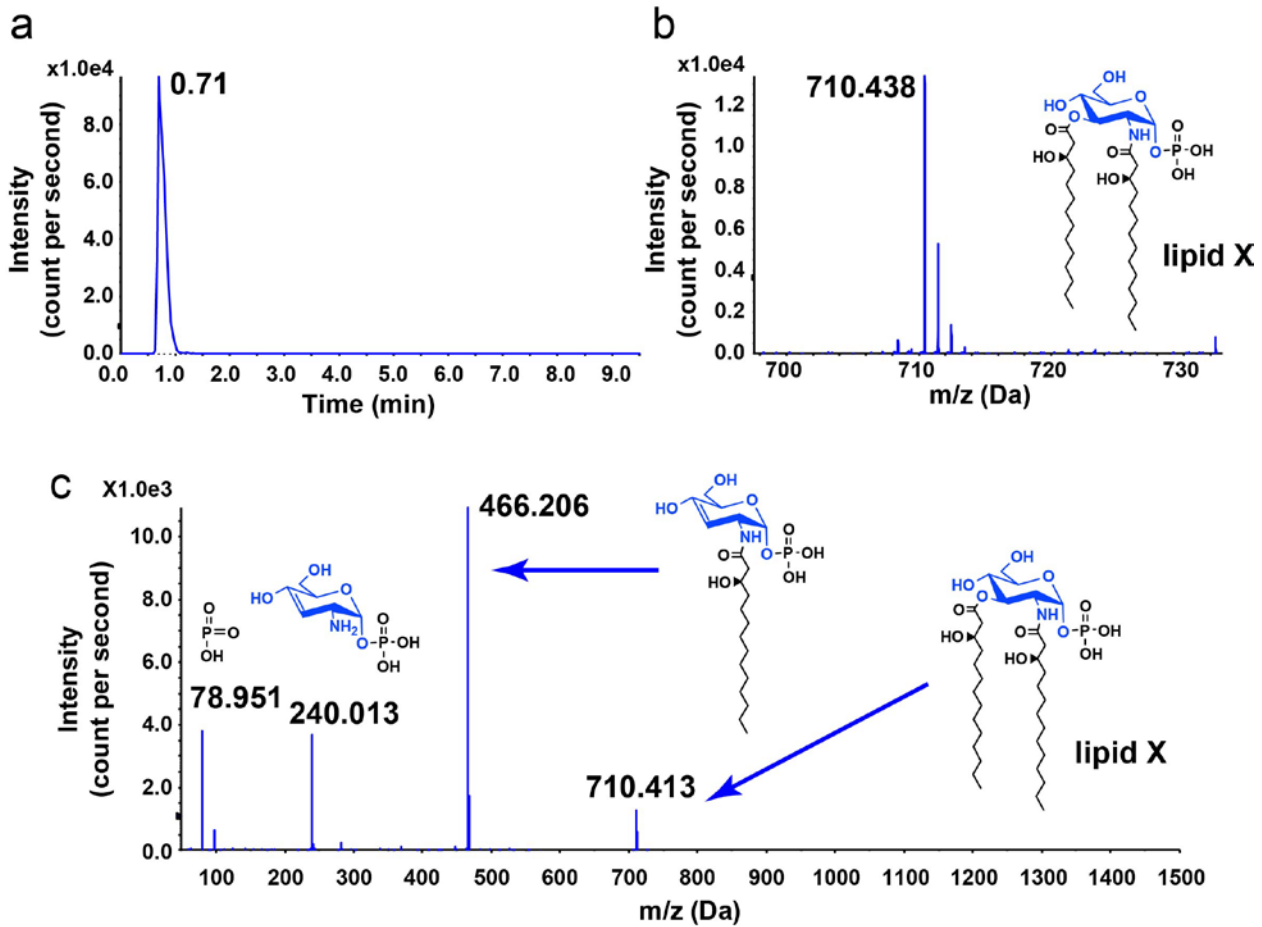
	Se-SAD	Native
Data collection		
Wavelength (Å)	0.97912	1.00000
Space group	R 3 2 :H	R 3 2 :H
Cell dimensions		
<i>a</i> , <i>b</i> , <i>c</i> (Å)	99.51, 99.51, 200.72	99.84, 99.84, 200.85
α , β , γ (°)	90, 90, 120	90, 90, 120
Resolution (Å)	79.19 - 2.80 (2.95 - 2.80)	79.42 - 2.55 (2.64 - 2.55)
R_{sym} or R_{merge}	0.077 (0.782)	0.052 (0.702)
Mean $I/\sigma I$	47.3 (6.0)	27.85 (4.67)
Completeness (%)	100 (100)	100 (100)
Redundancy	39.5 (40.4)	10.9 (11.4)
Total reflections	383381 (56298)	140558 (14302)
Unique reflections	9716 (1395)	12876 (1253)
SAD Phasing		
Figure of Merit (FOM)	0.416	
Refinement		
$R_{\text{work}} / R_{\text{free}}$		0.192/0.227
No. atoms		2004
Protein		1915
Ligand/ion		70
Water		19
Average <i>B</i> -factors		58.85
Protein		58.71
Ligand/ion		65.53
Water		48.61
R.m.s. deviations		
Bond lengths (Å)		0.004
Bond angles (°)		0.62
Ramachandran		
Favored (%)		97.5
Allowed (%)		2.5
Outliers (%)		0.0

*Values in parentheses are for highest-resolution shell.

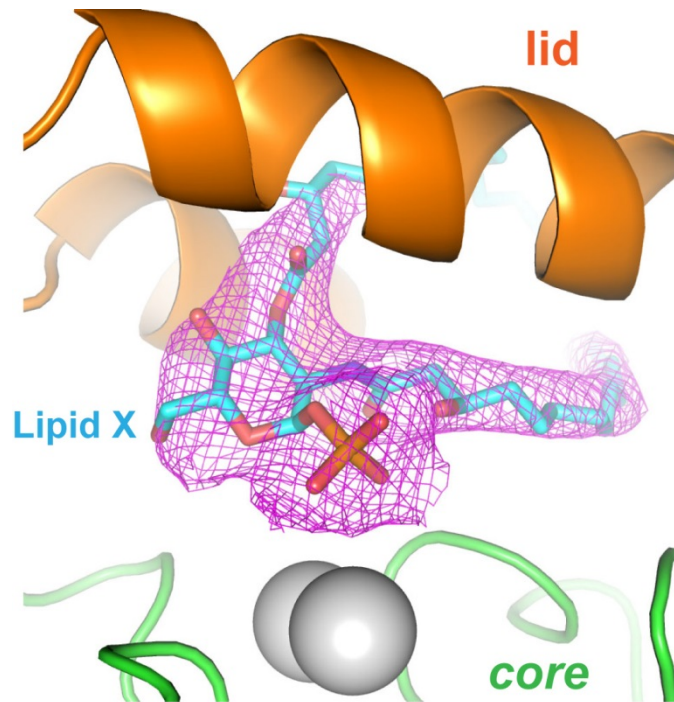
SUPPLEMENTARY FIGURES



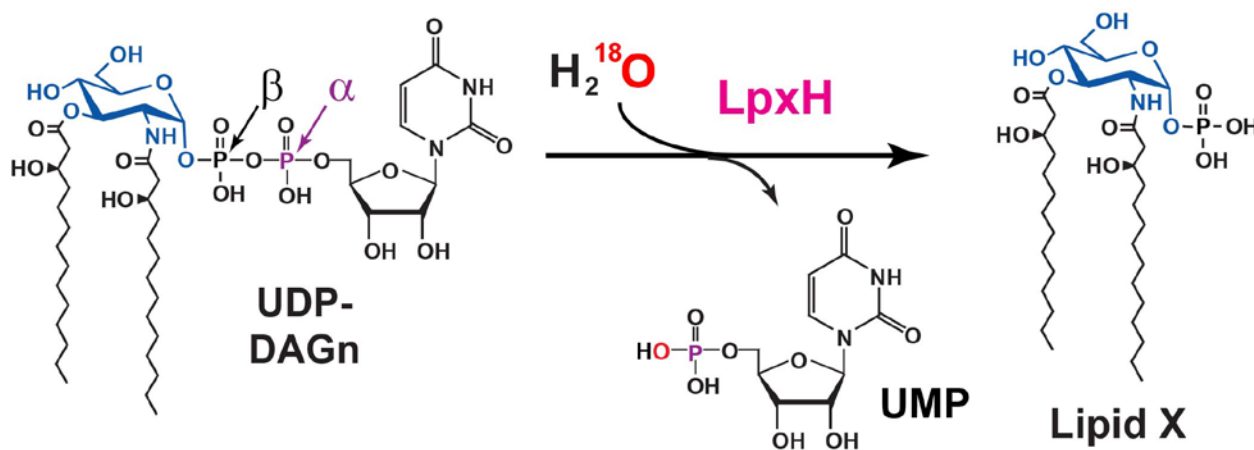
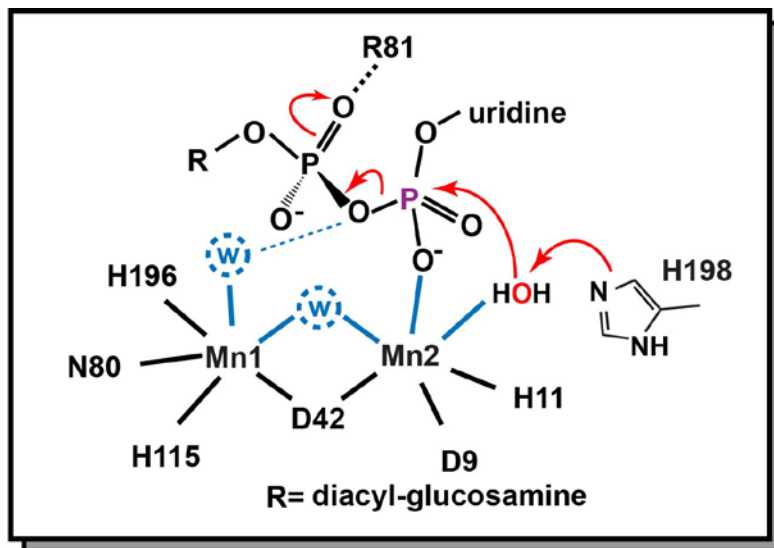
Supplementary Figure 1 | Lipid A biosynthetic pathway in *E. coli*. Cytosolic lipid A enzymes are colored in blue; membrane-associated enzymes are colored in magenta and orange; and the inner membrane enzymes are colored in purple. The UDP-2,3-diacylglucosamine pyrophosphatase LpxH (colored in magenta) is found in β - and γ -proteobacteria. Its functional orthologues, LpxI in α -proteobacteria and the recently identified LpxG in the Chlamydiae genus, are colored in orange.



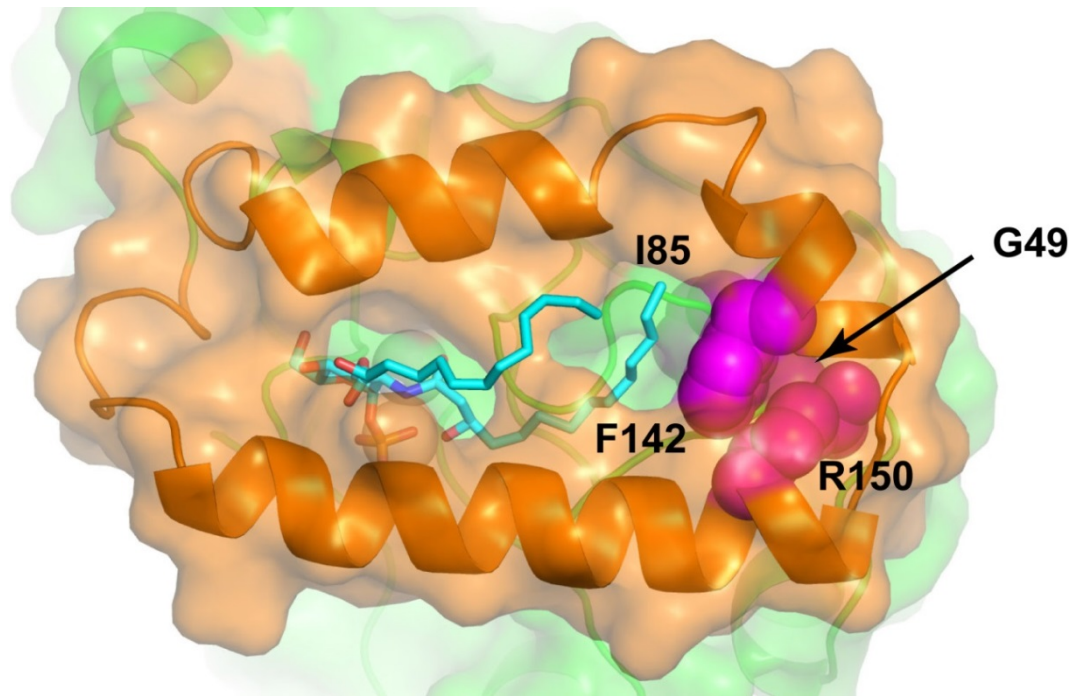
Supplementary Figure 3 | LC-MS analysis of the co-purifying lipid with LpxH. **a**, HPLC ion current profile monitored at m/z of 710.44. **b**, Mass spectrometry analysis of the extracted lipid reveals a major peak at m/z of 710.438, consistent with predicted mass of *E. coli* lipid X ($[M-H]^-$ m/z of 710.42). **c**, MS/MS analysis reveals components consistent with the fragmentation of lipid X. Results shown in the figure are representative of three biological and technical replicates.



Supplementary Figure 4 | Omit electron density map of lipid X. Purple mesh represents the $2mF_o-DF_c$ map contoured at 1.0σ calculated with lipid X removed from the structure.



Supplementary Figure 5 | Proposed mechanism of LpxH catalysis. LpxH hydrolyzes UDP-DAGn through a water-mediated attack on the α -phosphate group (purple) of the UDP moiety. Incorporation of the ^{18}O atom from heavy water is indicated in red. The proposed locations of Mn-chelating water molecules are based on analogy with other members of the CLP enzymes. In the proposed mechanism, the catalytic manganese ion (Mn2) polarizes a bound water molecule and assists the general base H198 in promoting the nucleophilic attack of the catalytic water molecule toward the α -phosphate group. Black and blue lines indicate observed and proposed metal interactions, respectively.



Supplementary Figure 6 | Resistance mutations of *E. coli* LpxH mapped onto the structure of HiLpxH. HiLpxH residues (G49, I85, F142 and R150) corresponding to resistance mutations of *E. coli* LpxH to a recently discovered inhibitor are shown as space-filling models. Lipid X is shown as the stick model and colored in cyan. The insertion lid and the core domain are shown as the ribbon diagram and their surfaces are colored in orange and pale green, respectively.